Improving on-wafer CD correlation analysis using advanced diagnostics and across-wafer light-source monitoring

Paolo Alagna[a], Omar Zurita[b], Greg Rechtsteiner[b], Ivan Lalovic[b]

Joost Bekaert [c],

a) Cymer LLC, Kapeldreef 75, 3001 Leuven, Belgium

b) Cymer LLC, 17075 Thornmint Court, San Diego, CA 92127

c) IMEC, Kapeldreef 75, B-3001 Leuven, Belgium

ABSTRACT:
With the implementation of multi-patterning ArF-immersion for sub 20nm integrated circuits (IC), advances in equipment monitoring and control are needed to support on-wafer yield performance. These in-situ equipment monitoring improvements, along with advanced litho-cell corrections based on on-wafer measurements, enable meeting stringent overlay and CD control requirements for advanced lithography patterning. The importance of light-source performance on lithography pattering (CD and overlay) has been discussed in previous publications.[1-3] Recent developments of Cymer ArF light-source metrology and on-board monitoring enable end-users to detect, for each exposed wafer, changes in the near-field and far-field spatial profiles and polarization performance, [4-6] in addition to the key 'optical' scalar parameters, such as bandwidth, wavelength and energy. The major advantage of this capability is that the key performance metrics are sampled at rates matched to wafer performance, e.g. every exposure field across the wafer, which is critical for direct correlation with on-wafer performance for process control and excursion detection.

In this work, we present a new technique for characterizing patterning impacts due to controlled changes in light-source optical parameters. This technique provides a significant improvement in characterization of patterning sensitivity and allows decoupling contributions from other process or equipment. Wafer patterning experiments have been carried out in imec facilities, using an XLR660i laser and NXT:1950i ASML scanner, with controlled changes to bandwidth, wavelength and energy performance within the wafer. The changes in patterning performance are characterized using scatterometry and top-down CD SEM, showing excellent correlations between light-source data and on-wafer CD and CD uniformity for typical patterning geometries for ~40nm half-pitch. The characterization technique discussed in this paper significantly improves the correlation quality between the light-source data and wafer patterning by increasing the measurement signal-to-noise. Finally, this paper discusses the requirements for improved light-source control for further shrink extensions of multiple-patterning ArF immersion lithography.

KEYWORDS: Excimer Laser, Bandwidth, Wavelength, Energy, Proximity Control, Optical Lithography, Focus, Dose, Resolution

1. INTRODUCTION:

ITRS technology roadmaps [7] show that ArF-immersion lithography solutions will continue to enable lithography patterning until EUV is fully adopted across patterning technologies. ArF-immersion multiple patterning with SMO (source-mask optimization), is considered complimentary to EUV to enable the definition of critical sub-20 nm technology.

The work we presented last year at the SPIE Advanced Lithography Conference[6], showed that near and far field beam characteristics can impact 1D patterning performance, as measured by the new laser on-board metrology developed by Cymer. This metrology enables monitoring near and far field beam performances (pointing, divergence) in addition to the polarization. In the same paper we showed pupil changes and on-wafer patterning impacts induced by controlled beam changes. The on-board metrology is part of the Cymer SmartPulse™ data product which additionally enables reporting key optical parameters, such as bandwidth, wavelength and energy per every exposure field on-wafer. This capability enables the direct characterization of patterning response on-wafer and comprehensive light source performance monitoring.

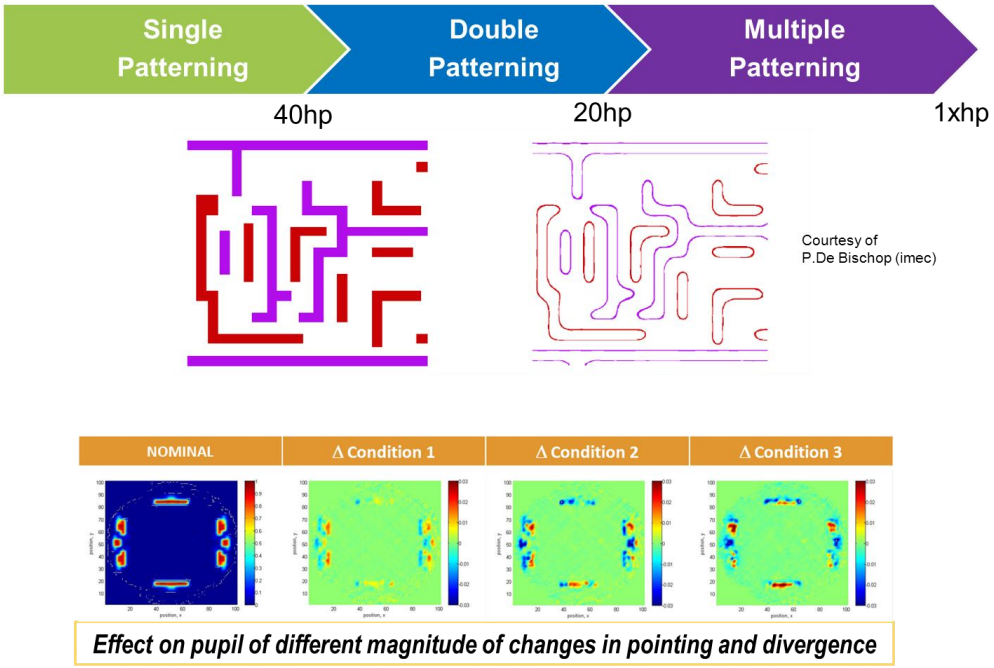

Figure 1. ITRS Summary of patterning transitions by half-pitch, example of multiple patterning logic layouts, and pupil response to laser induced changes [6].

Previous experimental results showed the importance of understanding of the ArF source impact on patterning performance during wafer exposure to ensure process stability. In order to enhance the characterization of specific patterning layer response, Cymer has developed an advanced technique which allows field level modulation of bandwidth, wavelength and dose stability across the wafer. This technique enables obtaining an accurate on-wafer response of 1D and 2D patterns to changes in laser performance, achieving a significant improvement in measurement signal to noise by removing the contribution of wafer-to-wafer measurement errors.

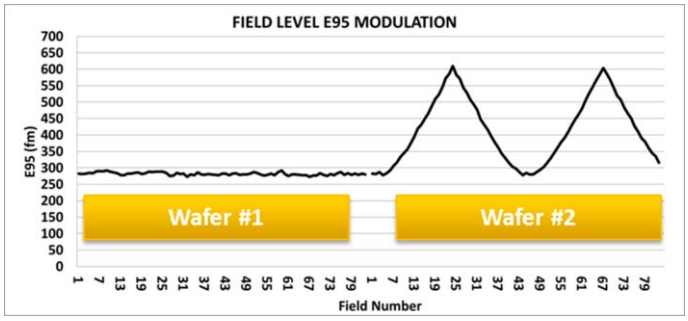

Figure 2. Example of Nominal Wafer Exposure (Wafer #1) and Field-to-field Laser Bandwidth E95 Modulation (Wafer #2)

2. PROCESS SENSITIVITY CHARACTERIZATION

The experimental activities reported in this paper were performed on the XLR 660ix laser feeding the NXT:1950i ASML scanner, installed in imec's 300mm facility. This system is interfaced with the Cymer SmartPulse^{TM} data product enabling per wafer and per field data for light-source performance obtained during the actual exposure of test wafers. The response to changes in bandwidth (E95) of 1D patterns with different line-width and pitch combinations was investigated first. Two sets of wafers were exposed: the first one at nominal bandwidth (300 fm), while the exposure of the second one is characterized by a change in E95 from nominal up to 600 fm. The bandwidth changes are modulated per exposed field, following a set of programmed set-points as described in Table 1.

Given that the imec infrastructure offers several different advanced metrology solutions, our selection has been made considering that we wanted to achieve high density of across wafer sampling, including intra-field (104 points per each 26mm x 33mm exposure) across the entire wafer (83 fields). Considering the high measurement density, we decided to use the scatterometry system (ASML YS-200), which is capable to achieve up to 107 measurements per minute (one pitch and one orientation) per wafer sample within reasonable tool time. Table 1 also includes the selection of the CD/pitch combinations. The process for the exposure of the scatterometry targets was already defined by imec : JSR AIM5484 resist at 105nm and the annular source with 1.35 NA, inner sigma of 0.79, outer sigma of 0.84 . The first scheduled test was conducted, modulating bandwidth (E95) across the wafer. Starting from nominal condition, each field has been exposed with a different setting.

TARGET CD

Mask Pitch 84nm CD 39 → Wafer CD 41nm
Mask Pitch 92nm CD 45 → Wafer CD 47nm
Mask Pitch 128nm CD 62 → Wafer CD 49nm
Mask Pitch 200nm CD 84 → Wafer CD 49nm
Note : No assist features

METROLOGY

Scatterometry (ASML-YieldStar 200)
Measurements per wafer : 8.632
(one pitch and orientation)

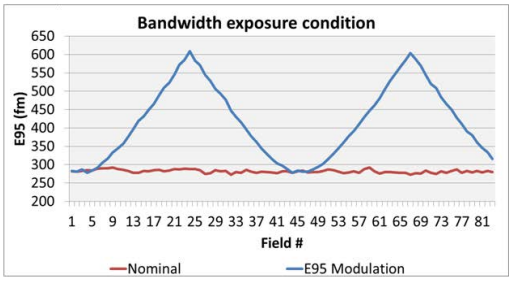

Table1. Measurement targets and exposure condition

The response of the four selected targets in Figure 3 shows, as expected, that the most contrast sensitive patterns (pitch 128 and pitch 200) exhibit a much higher CD response [1-3] to changes in laser bandwidth. This first test shows the importance of field level data collection; the dashed line in Figure 3 shows the average wafer CD of the modulated wafer from the CD average of the nominal wafer. The histogram bars, on the other hand, show the CD differences per field between the nominal wafer condition and exposures where field-level changes in E95 were present. From these plots it is immediately clear how important field level data is to enhance the yield control capability. This figure shows also the direct correlation between the bandwidth changes achieved per field and impacts on different type of 1D pattern on wafer.

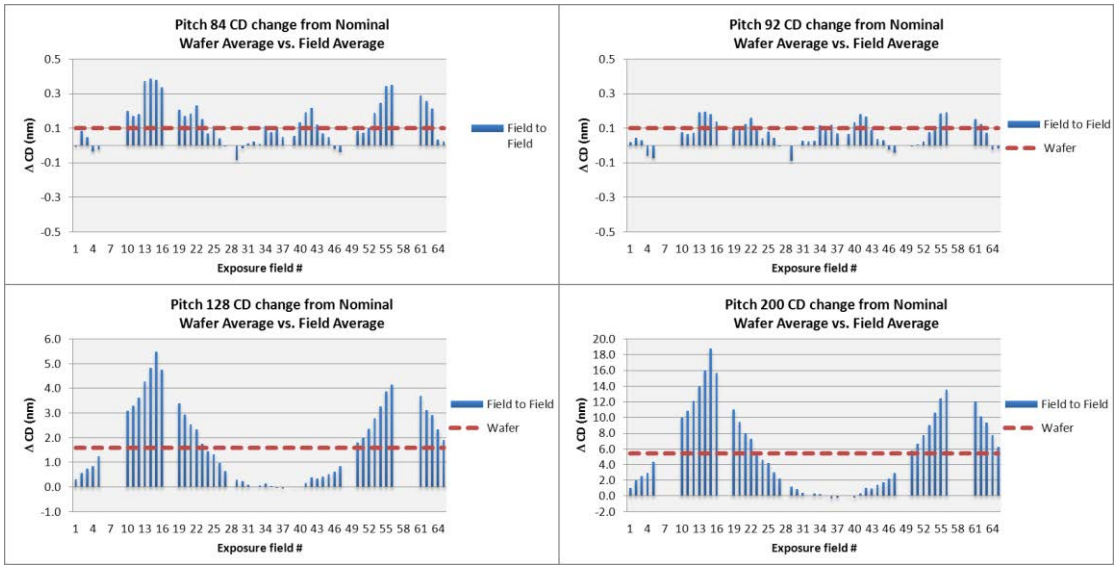

Figure 3. Field to field CD response to bandwidth changes. Difference from nominal condition. Edge field removed.

Characterization of 1D pattern response by changing laser bandwidth performance per exposure field confirms the quadratic response for all CD-pitch combinations, as has been already reported in previous work [1-3]. Additionally this analysis can be used to qualify the precision of laser bandwidth data reporting, which shows excellent agreement with scatterometry on-wafer measurements, with R^2 exceeding 0.99 for the most sensitive pitches (pitch 128nm and 200nm).

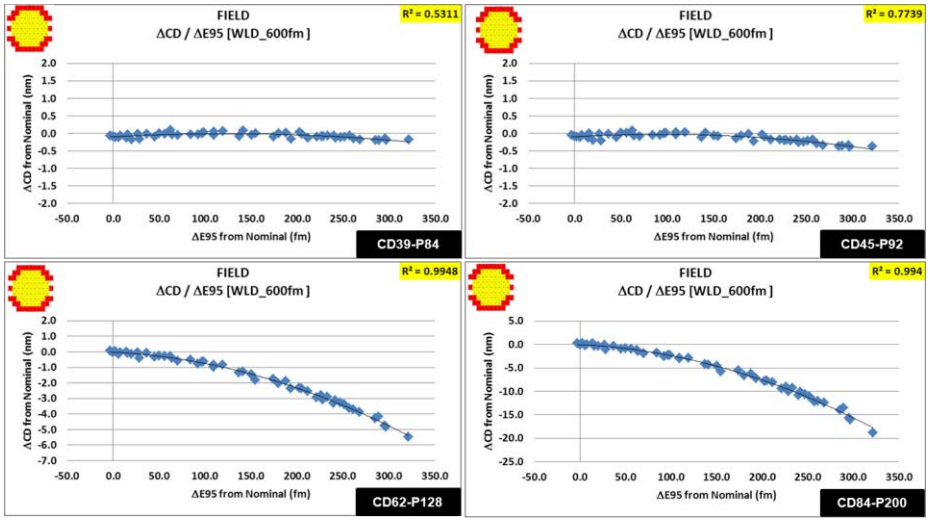

Figure 4. Different line-width/pitch combinations show a common trend.

We also quantified the changes in line-width roughness induced by optical parameter's changes. Contrast changes, as induced by variation of laser bandwidth, is only one of the factors which can contribute to changes in pattern roughness, and the interactions are indeed more challenging to investigate than simply the line-width CD response. We applied the same approach to vary the laser bandwidth performance across the wafer to directly quantify the roughness response through a range of different E95 performance levels. The investigation of the line-width roughness response has been conducted on a different reticle enabling lines and spaces that can be also cleaved for cross-section analysis. An optimized source, which improved the overall roughness, has been also implemented (x-polarized, dipole 40 degree, Y orientation with 1.35 NA, inner sigma of 0.70, outer sigma of 0.80). Figure 5 shows an example of what was the response to a pattern with a line-space rate of 1:2. The measurements were executed by the CD-SEM Hitachi CG5000.

In the left-hand graph in Figure 5, the change in line-width roughness also follows a 2nd order polynomial fit to bandwidth E95 performance; this is consistent with an excellent paper on resist characterization published previously[8].

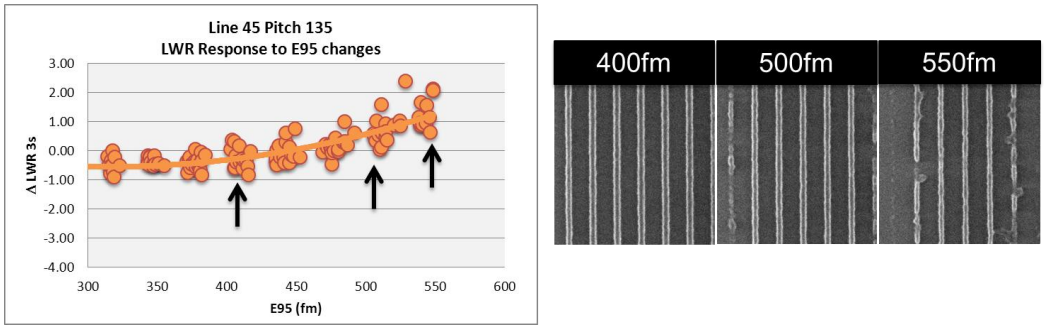

Figure 5. LWR Change as Function of Different E95

The per field changes in laser performance have been applied to experimentally measure the pattern response to additional laser optical parameters, including wavelength and energy stability. Figure 6 shows the summary of the laser actuation conditions and wafer patterning results.

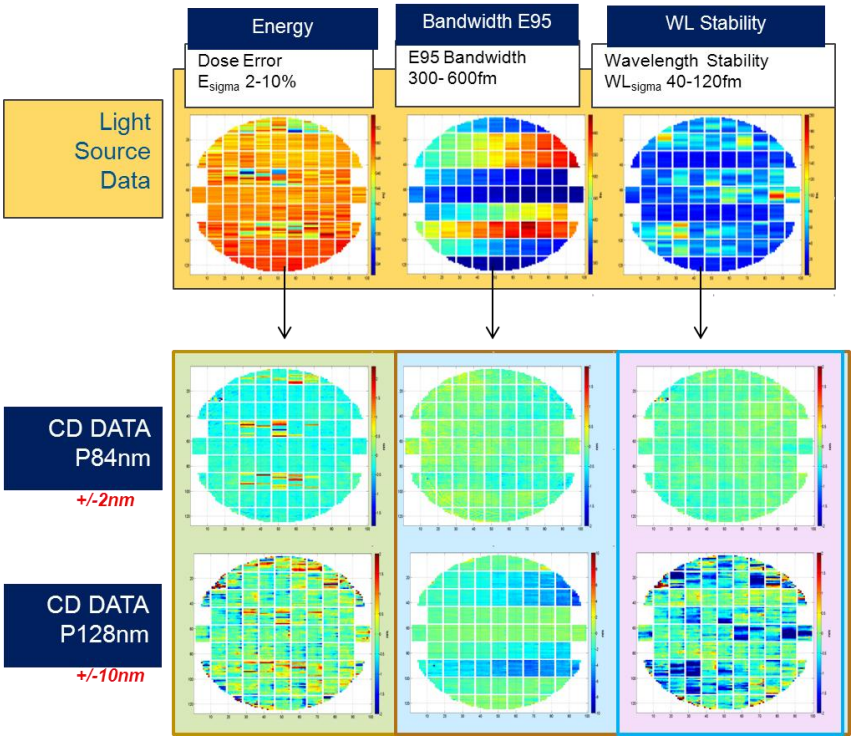

Figure 6. Across-wafer 1D Pattern response to per-field modulation of optical laser parameters

The methodology applied here demonstrates that the response of 1D pattern is well correlated to programmed changes in laser parameters across the wafer.

We also investigated the more complex response that results from 2D patterns, which are more representative of the response of actual device features. We selected to use as reference the first split of a double patterning 14nm logic Metal 1 process layer, which is part of one of imec's process development test vehicles. The response of three different types of patterns has been measured for this part of the experiment. Our attention was particularly dedicated to the response of the

critical hotspots and tip-to-trench and tip-to-tip structures. Wafer samples were prepared with a stack made by 100 nm of SOC (Spin On Carbon) and 40 nm of SOG (Spin on Glass), then coated with 100 nm of Fujifilm M190 resist (negative tone development process), using an optimized freeform source.

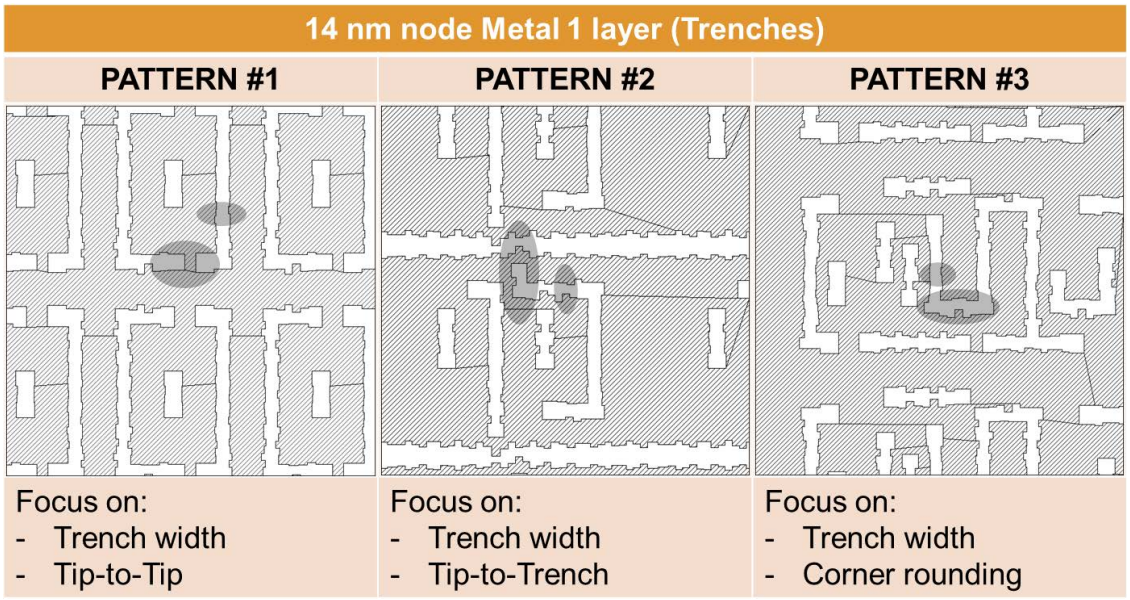

Figure 7.2D Mask Pattern Layouts Selected from imec double-patterning 14nm logic Metal 1 layer (first split)

The pattern sensitivity study on 2D structures requires a more structured approach[9,10]; the analysis has been focused then in different areas:

a. 1D trench width measurement distribution

b. 2D critical features changes

c. Contour analysis

d. Defect density analysis

Critical dimension measurements were performed on Hitachi CG5000 CD-SEM. Each value reported in the plots is the average of 4 identical patterns located in the exposure field.

a. 1D CUT-LINE-MEASUREMENT CHANGE

The trench width measurements from 2D layouts can lose part of the predictability characteristics, unlike to what has been seen in the 1D structure [Figure 4].This is mainly caused by the fact that the pattern definition could be somehow modified by the optical proximity interactions with other patterns (lines or line ends), OPC corrections and mask-writer errors. Figure 7 shows the measurement change of a single orientation line width in a complex 2D structure mainly keep the same quadratic response as shown in the L/S 1D pattern measured using scatterometry previously.

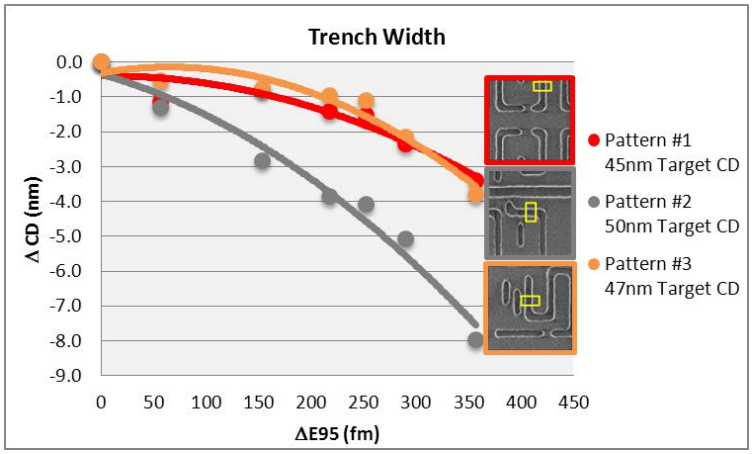

Figure 7. Trench width measurement changes at different bandwidth conditions

The target CD for these features (after etch) is approximately 32 nm, so if we assume a 10% CD error tolerance, the litho specification on the CD is ± 3.2 nm. In this scenario, bandwidth changes in the range of 100fm can contribute to a significant part of the total available budget for Metal 1 patterns.

b. TIP-TO-TIP AND TIP-TO-TRENCH MEASUREMENT CHANGES

2D patterns offer indeed a much wider combination of critical features with respect to the single orientation pattern. The measurement of the distance between two opposite line ends (tip-to-tip) or between a line-end perpendicular to a trench (tip-to-trench) were also obtained as function of different bandwidth. Plotting the tip-to-trench or tip-to-tip distance (or gap) for each change in bandwidth (from nominal 300fm) (Figure 8), it is evident that the sensitivity of line-ends can be much more unpredictable.

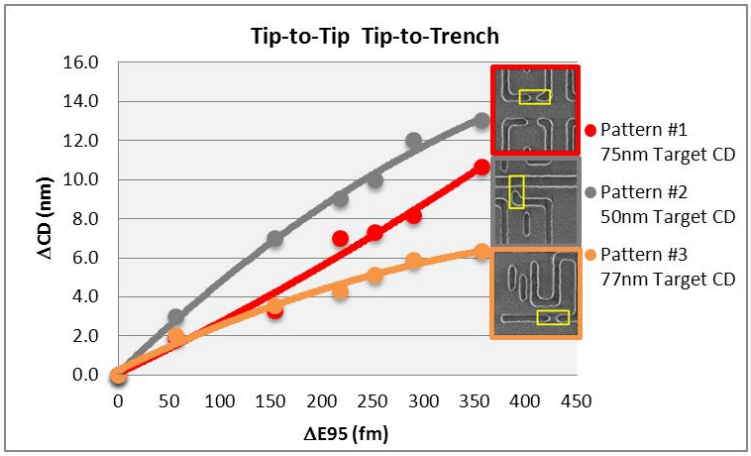

Figure 8. Tip-to-Tip and Tip-to-Trench measurement changes at different bandwidth conditions

Trying to define the best analysis approach in cases like the one we are considering, has been decided to plot the ratio between measurement changes in GAPS (tip-to-line or trench) and TRENCH WIDTH as function of different

bandwidth (E95) variations. As reported in the results summarized in the following figure the sensitivity of line-ends can be up to 4 to 5 times higher compared to single orientation trench-width measurement for Metal 1 patterning.

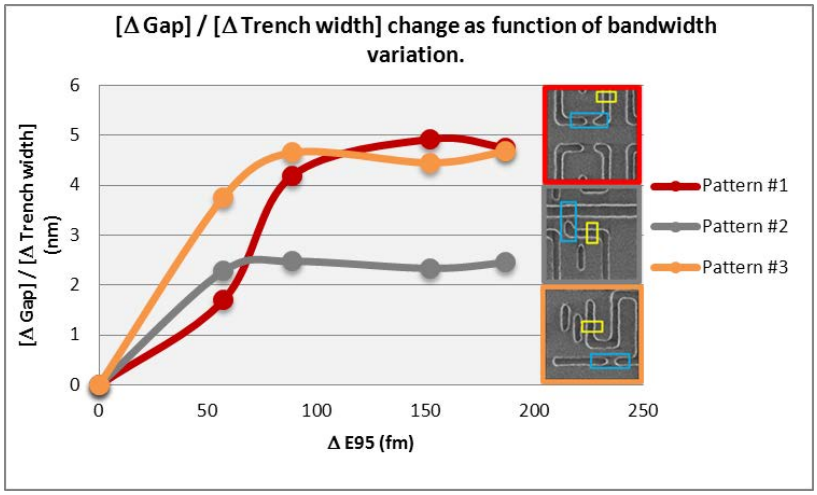

Figure 9. Correlation between changes in the gap distances and trench width as function of E95 change

c. CONTOUR ANALYSIS

The characterization of 2D patterns is indeed challenging because the complexity of the process factors related to such structures (OPC, process stack, proximity, hotspots, etc.) leave even to the most advance stochastic approach an important margin of uncertainty. In our experiment we have chosen to analyze those critical features also by using contour analysis of SEM measured patterns. We used the capability available in the Hitachi Hi-frame platform to superimpose the measured contours with the reticle design file (GDS). We averaged four measurements per field at the same laser bandwidth condition, and the extracted contour results are shown in Figure 10.

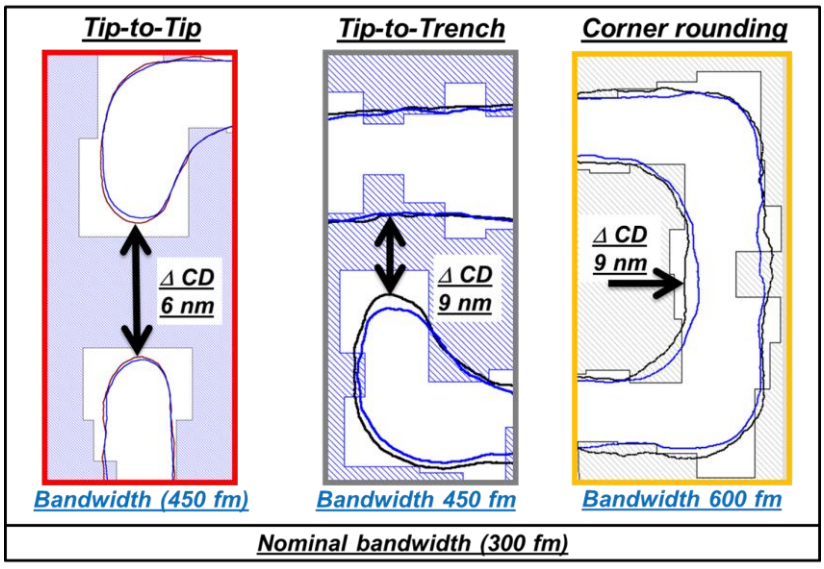

Figure 10. Contour Analysis of Experimental CD contours using Hitachi Hi-frame

Even though maximum changes allowed for the tip-to-tip and tip-to-trench would be larger (imec specifies 9nm and 6nm control respectively); as shown, the maximum laser E95 excursion up to 600fm would significantly exceed the

allowed performance of trench-ends. No specific criteria are defined for the corner rounding, however the impacts due to contrast loss can clearly impact 2D layout critical areas.

d. DEFECT DENSITY ANALYSIS

We also carried out a defect density analysis to determine the potential impact of bandwidth change on 2D structures. Using KLA 2825 optical inspection tool we inspected the field area where the different modules selected in this experiment where located resulting in an overall scanning area of 69.69 cm^2 (57 exposure fields scanned). Our objective was to benchmark the defect density distribution of 4 different exposure conditions: Nominal (reference) bandwidth wafers, 300fm to 600fm of E95 bandwidth per-field modulation across the wafer (labeled BW1), Nominal bandwidth and 2% of dose error (fixed in all wafer), Nominal bandwidth and large dose error (> 20%). Multiple wafers were exposed, including four reference wafers and two wafers per experimental condition, to obtain a measure of the wafer-to-wafer reproducibility. Figure 10 shows that the defect density (total defect count per 69.69 cm^2 area) increases by as much as 25 times for the wafers exposed with bandwidth modulation compared to the Nominal wafer exposures. The additional dose error conditions increase the defect density further, as expected.

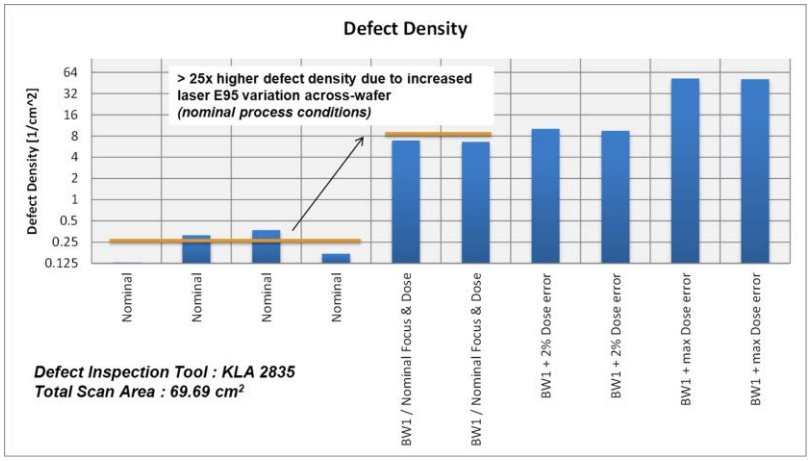

Figure 11. Defect Density as a Function of Different Experiment Conditions

3. ADVANCE SOURCE MONITORING CAPABILITIES

Given the implementation of multiple patterning, advances in equipment monitoring and control are needed to support on-wafer yield and process development cycle-time. In previous work[4-6], the Cymer Smartpulse™ platform capabilities have been described in order to meet the needs of advanced lithography patterning control. This capability is used by chipmakers to enhance equipment monitoring, providing key light-source performance data for each exposed wafer. SmartPulse ™ enables direct correlation of light source performance with wafer exposure data, and includes per field sampling-rate data for key optical parameters (bandwidth, wavelength and energy). As shown in this paper, per field sampling and high level of metrology precision (quality) is required for accurate correlation and determination of patterning impacts.

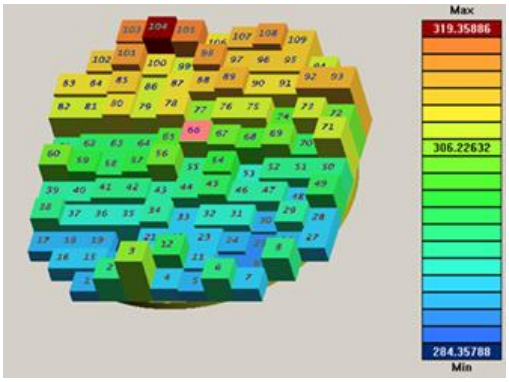

Figure 11. SmartPulse™ Field-level Wafer Exposed Data

4. CONCLUSIONS

The on wafer impact of light source optical parameters modulation have been characterized using an advanced laser experiment at imec's facilities in Leuven (BE). This technique allowed us to measure the lithographic response of 1D patterns with different line-width and pitch combinations, through field level modulation of wavelength, dose error and bandwidth (E95). The results obtained are consistent with what has been reported in the literature [1-3] showing a quadratic correlation between bandwidth and line-width change; roughness changes showed also a similar response. The same approach has been used to characterize wafer patterning performance to E95 changes, on three samples of the first split of a double patterning 20nm logic Metal 1 process layer. Despite the trench-width measurements were consistent with the expectations, it must be taken into account that in the examples considered, due to the optical proximity interactions with other patterns (lines or line ends), OPC corrections and mask-writer errors the predictability is not as clear as in the 1D pattern. With the technique adopted it was also possible to study the overall 2D pattern modification to E95 changes. In particular our study showed how the distance change between two opposite trench ends (tip-to-tip) or between a trench-end perpendicular to a trench (tip-to-trench) can be up to 4 times higher than the critical line-width present in the same structure, when a deviation of 100 fm from nominal bandwidth condition, is measured. Observing the results change we could conclude that 150 fm of E95 change from standard working conditions can significantly compromise the yield, causing remarkable changes in the trench-width and trench-ends patterning results. Defect analysis showed that the defect density on wafers where the bandwidth field level modulation has been applied, if up to 25 times higher than wafers exposed in nominal condition. In this experiment we have also demonstrated that per field sampling and high level of metrology precision (quality) is required for accurate correlation and determination of patterning impacts and that SmartPulse^{TM} enables direct field level correlation of light source performance with patterning data, for key optical parameters.

ACKNOWLEDGEMENTS

The authors are very grateful for all support given to this project. In particular,Remo Petrella of Cymer, Koen D'Havé, Peter De Bisschop, Jing Wang, Wouter Pypen, Frieda Van Roey of imec, Kei Sakai, Daisuke Fuchimoto from Hitachi, Yves Belien, Charles Schaap together with all ASML on-site support team in imec, are acknowledged for their help, practical discussions and organizational support.

REFERENCES:

[1] U. Iessi ed al. "Laser bandwidth effect on overlay budget and imaging for the 45 nm and 32nm technology nodes with immersion lithography", Proc. SPIE 7973, Optical Microlithography XXIV, 797328

[2] N. Seong, et al. "Analysis of the effect of laser bandwidth on imaging of memory patterns", Proc. SPIE 7140, Lithography Asia 2008, 714042

[3] P. De Bisschop et al. "Impact of finite laser bandwidth on the CD of L/S structures", Journal of Micro / Nanolithography, MEMS and MOEMS (JM3), Vol. 7, No. 3 (2008)

[4] T. Cacouris et al. "Advanced light source technologies that enable high-volume manufacturing of DUV lithography extensions" SPIE Proc. Vol. 8326 (2012)

[5] J.Choi et al., "Enhancing lithography process control through advanced, on-board beam parameter metrology for wafer level monitoring of light source parameters", Proc. SPIE Optical Microlithography XXV 8326,99 (2012).

[6] P.Alagna et al., "Lithography imaging control by enhanced monitoring of light source performance",Proc. SPIE Optical Microlithography XXVI 8683,28 (2013)

[7] ITRS, International Technology Roadmap for Semiconductors [www.itrs.net]

[8] Pawloski et al., "Characterization of line edge roughness in photoresist using an image fading technique", Proc. SPIE Optical Microlithography XXI, 5376-44 (2004)

[09] K. Iwase et al. "A new source optimization approach for 2X node logic" , Proc. SPIE. 8166 Photomask Technology 2011

[10] J. Bekaert et al. "Freeform illumination sources : an experimental study of source-mask optimization for 22-nm SRAM cells" Proc. SPIE 7640, Optical Microlithography XXIII, 7640,08 (2010);

Flexible Power 90W to 120W ArF Immersion Light Source for Future Semiconductor Lithography

R. Burdt, T. Duffey, J. Thornes, T. Bibby, R. Rokitski, E. Mason, J. Melchior, T. Aggarwal, D. Haran, J. Wang, G. Rechtsteiner, M. Haviland, D. Brown
Cymer, Inc. (United States)

ABSTRACT

Semiconductor market demand for improved performance at lower cost continues to drive enhancements in excimer light source technologies. Increased output power, reduced variability in key light source parameters, and improved beam stability are required of the light source to support immersion lithography, multi-patterning, and 450mm wafer applications in high volume semiconductor manufacturing. To support future scanner needs, Cymer conducted a technology demonstration program to evaluate the design elements for a 120W ArFi light source. The program was based on the 90W XLR 600ix platform, and included rapid power switching between 90W and 120W modes to potentially support lot-to-lot changes in desired power. The 120W requirements also included improved beam stability in an exposure window conditionally reduced by 20%. The 120W output power is achieved by efficiency gains in system design, keeping system input power at the same level as the 90W XLR 600ix. To assess system to system variability, detailed system testing was conducted from 90W – 120W with reproducible results.

1. INTRODUCTION

Cymer first introduced the XLR 500i light source with master oscillator – power regenerative amplifier (MOPRA) architecture in 2007 to meet light source requirements primarily on cost-of-ownership and dose stability [1]. The 6000Hz, 60W XLR 500i enabled improved resolution and critical dimension (CD) control at high throughput, with reduced operating costs. Subsequent light source models offered by Cymer and based on the dual-chamber MOPRA architecture, include the XLR 600i introduced in 2008 [2], and the XLR 600ix introduced in 2009 [3]. These light sources enabled further improvements in the resolution of semiconductor lithography past the 32nm node, through the use of double patterning and the extension of numerical aperture to 1.3 and beyond. Power output of the XLR 600ix increased by 30% from the XLR 500i to 90W, and beam stability requirements were tightened to enable scanner improvements in focus and overlay associated with multiple patterning. The XLR 600ix light source has demonstrated excellent system performance stability over a 30 billion pulse lifetest [4], and over 200 systems in the field supporting memory, logic, and foundry applications have demonstrated stable and reliable performance with greater than 99.6% uptime [5].

To support reductions in critical dimension and a transition to 450mm wafer size, the semiconductor roadmap demands further improvements in scanner resolution and throughput, which in turn places requirements on the light source for higher output power and tighter beam stability in a reduced exposure window. Furthermore, the flexibility in scanner operating parameters demanded by multi-patterning techniques, creates requirements on the light source to quickly switch between and control beam stability at different wavelengths, bandwidths, and pulse energies. To prepare for future scanner requirements, Cymer has conducted a technology demonstration program to evaluate the design elements for a 120W ArFi light source. The program was based on the 90W XLR 600ix platform, and included rapid power switching between 90W and 120W modes to potentially support lot-to-lot changes in desired power. Three 120W ArFi demonstration units were built and tested, and were identical in configuration. The increase in output power from 90W to 120W was realized by utilizing efficiency gains in

multiple system components in a manner that does not increase the system input power. All dose stability and wavelength stability metrics for the 120W ArFi demonstrators are processed in an exposure window reduced by 20% as compared to the XLR 600ix, reflecting the higher stage speed expected in future scanners. To accommodate diverse lithography process conditions, the light source output power, wavelength, spectral bandwidth, and duty cycle can all be varied over a wide range.

This manuscript reports on the specific advancements in technology that enable stable system performance of the 120W ArFi demonstrators. Data will be shown for three systems that were tested to clarify the system to system variation that can be expected when operating at higher power. These data will include light source performance metrics in a test meant to simulate wafer exposure firing patterns in 90W and 120W modes, and in a long-duration stress test meant to characterize performance across the vast majority of possible firing modes.

2. TECHNOLOGY ADVANCEMENTS ENABLING FLEXIBLE 90W TO 120W OPERATION

The output of the 120W ArFi light source demonstrators will be pulses of light with temporal duration between 100 and 150ns, at a repetition rate at or less than 6000Hz. For continuous firing at the maximum repetition rate, 15mJ pulse energy results in 90W output power, and 20mJ pulse energy results in 120W output power. The 120W ArFi light source is capable of firing at any pulse energy between and including 11.7mJ to 23.0mJ. The central wavelength of the light source is 193.3680nm, and a typical spectral bandwidth is 300fm using the integral-95% definition (hereafter referred to as 'E95% bandwidth'). The central wavelength and E95% bandwidth of the 120W ArFi light source are actively controlled to support light source requirements derived from the focus, overlay, and CD control requirements of the scanner. Spectral parameters are also tunable to support precise matching of the light source spectrum to diverse lithographic tools. The size of the output beam, as defined within the full-width-5% of the near-field intensity distribution, is 12mm by 12mm, divergence in two axes is less than 2mrad, and the peak beam energy density is less than 40mJ/cm^2 for all operating conditions up to 120W.

The system architecture of the 120W ArFi light source demonstrators is a dual-chamber configuration based on the field-proven XLR 600ix, to take advantage of high uptime demonstrated by over 200 XLR 600ix sources operating in the field [5]. A simplified diagram of the light source with some core modules identified is shown in Figure 1. The master-oscillator subsystem (module 2) creates a low energy pulse of light with short temporal duration (10s of ns) and precise control of spectral parameters. This light pulse traverses relay optics and metrology modules, then enters the power regenerative amplifier (module 3). The ring optics (module 4) send the light pulse through many passes of the power regenerative amplifier as energy of the light pulse is amplified consistent with desired light source output power. Finally, the temporal duration of the light pulse is increased by the optical pulse stretcher (module 5) in order to reduce peak irradiance of the beam, thereby extending lifetime of scanner optics. Driving a precisely-timed electrical discharge in both the master-oscillator and in the power regenerative amplifier to provide laser gain, are a series of solid-state pulsed power modules (module 1).

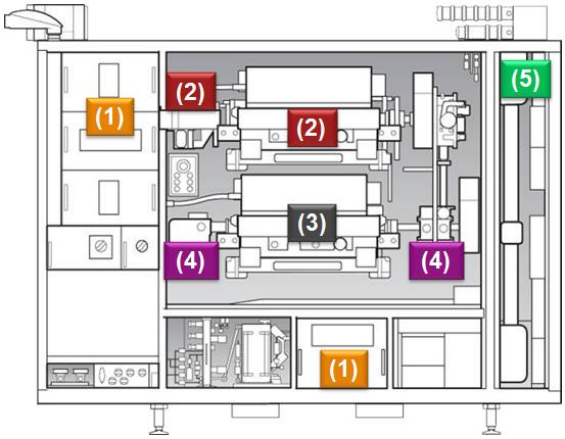

Figure 1. Diagram of the XLR 660ix / 120W ArFi light source with some core modules labeled: (1) solid-state pulsed power modules, (2) master-oscillator subsystem, (3) power regenerative amplifier, (4) ring optics, (5) optical pulse stretcher.

Most of the XLR 600ix core modules and their operating conditions see no change from the XLR 600ix to the 120W ArFi light source. All of the solid-state pulsed power modules (module 1 in Figure 1) and their operating conditions are unchanged in the 120W ArFi light source. The master-oscillator subsystem (module 2) is also unchanged in design and operating conditions. The power regenerative amplifier is largely based on the design used in the XLR 600ix, with a few key improvements that enable reduced optical losses and increased laser gain. The ring optics are also optimized for reduced optical losses, and additional improvements were made to ensure beam stability from 90W to 120W. Fast power switching on lot-to-lot timescales is achieved by the automated use of intracavity attenuating elements in the ring optics. Additionally, improvements were made to the optical pulse stretcher (module 5) to ensure beam stability at the increased thermal load of the 120W light source.

Inputs to the light source from facilities include cooling water, electrical power, optics purge gas, and the chamber gas mixture. From the point-of-view of facilities input to the light source, there is no difference between the XLR 600ix light source and the 120W ArFi light source. All water, electrical, purge gas, and chamber gas requirements are unchanged. The reduced optical losses and increased laser gain of the power regenerative amplifier subsystem (modules 3 and 4) enable the 30% increase in output power with no impact to system input power, i.e., the wall-plug efficiency of the 120W ArFi light source is 30% higher as compared to the XLR 600ix. Figure 2 quantifies the increase in stable 193nm output power per kilowatt of input power over three generations of Cymer light source, up to the 120W ArFi tool.

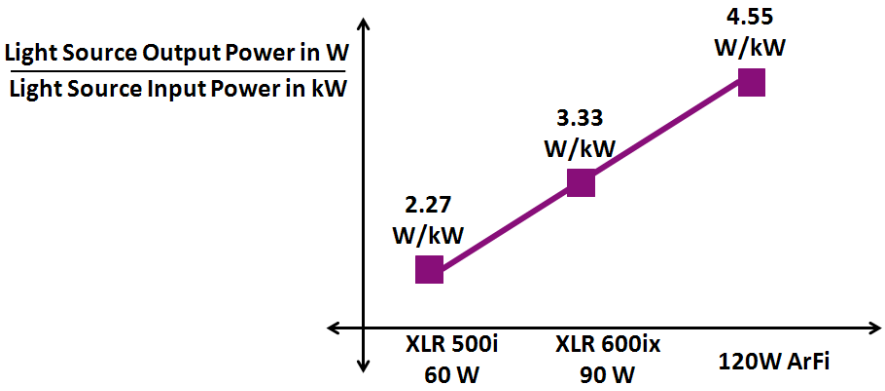

Figure 2. Wall-plug efficiency, as measured at Cymer San Diego, over three generations of Cymer light source.

3. SYSTEM PERFORMANCE DATA FOR THREE LIGHT SOURCES

Three 120W ArFi light sources were built in 2013 as a technology demonstration. A suite of extensive design validation tests was executed and passed for each 120W ArFi light source. This test suite fires the light source in the vast majority of its possible use cases, and monitors all performance metrics of concern to chipmakers on the equivalent of a die-by-die basis. Additional tests were run to validate the design intent of all changes in the 120W ArFi design from the XLR 600ix, and results validated the efficacy of improvements made to the power regenerative amplifier and ring optics to improve efficiency and allow lot-to-lot power switching.

Data from two tests within this extensive test suite will be presented. Data will be shown from the *Wafer Simulation Test*, designed to replicate firing patterns used in 90W and 120W wafer-exposure modes, and also to monitor system performance across lot-to-lot power switching. Data is also presented from the *20-Hour Endurance Test*, meant to fire the light source in the majority of its possible use cases while monitoring all light source performance metrics.

Dose stability is a measure of the output power stability, used to ensure uniform irradiation of the photo-resist, and is shown in Figure 3 as measured in the wafer simulation test for three Cymer 120W ArFi light sources. The test includes three 90W firing modes, and three 120W firing modes, with a power switch executed after each mode. The data demonstrate consistent system performance for three light sources, with system-to-system variability almost within the die-to-die variability for an individual light source. Whereas the data of Figure 3 show system performance across a few simulated wafer exposure modes lasting about 3 minutes, the data of Figure 4 show data across 10 hours of firing in 90W modes, then 10 hours of firing in 120W modes. Each trace in Figure 4 represents approximately 70 thousand data points, where each data point represents a light source performance metric derived from a single burst fired by the light source (total number of light pulses in the 20-hour test is approximately 70 million). The 90W and 120W modes of the 20-hour test are nominal power levels; the actual power levels depend on the light source pulse energy and duty cycle. The 20-hour test uses pulse energies from 11.7mJ to 17.3mJ at the 90W mode, and from 15.5mJ to 23.0mJ at the 120W mode, demonstrating the ability of the light source to fire between 90W and 120W, and to fire at overlapping energy targets in both nominal power modes.

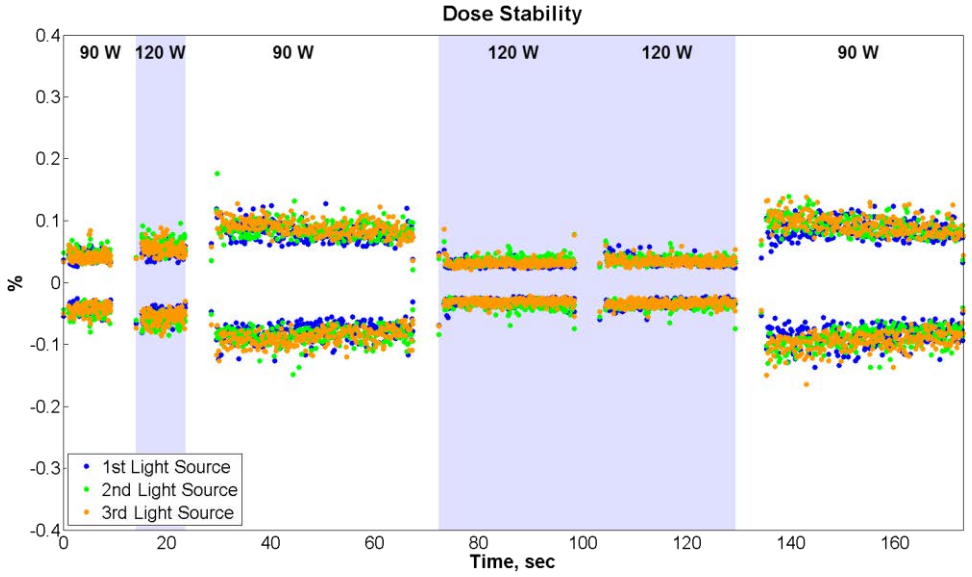

Figure 3. Dose stability of three light sources in the Wafer Simulation Test, demonstrating stable and consistent system performance for 90W and 120W power modes across lot-to-lot power switching.

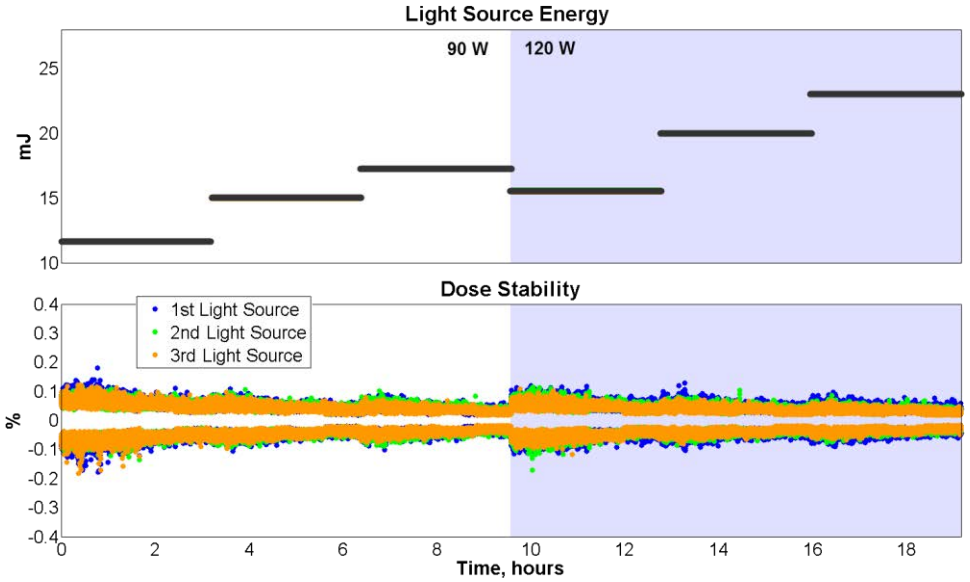

Figure 4. Light source energy and dose stability of three light sources in the 20-Hour Endurance Test, demonstrating stable and consistent system performance for 90W and 120W power modes.

The wavelength and E95% bandwidth of the 120W ArFi light source are actively controlled in order to support anticipated focus, overlay, and CD control requirements of the scanner. Figure 5 shows wavelength and bandwidth stability data for three light sources collected in the wafer simulation test; Figure 6 shows the same for data collected in the 20-hour endurance test. For both cases, multiple light sources demonstrate stable and consistent wavelength and bandwidth system performance in 90W and 120W modes.

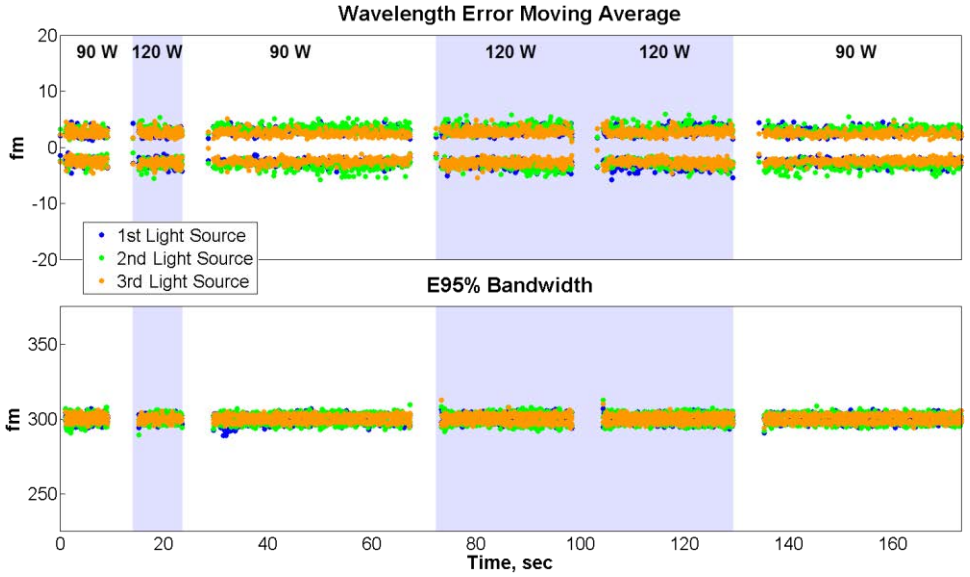

Figure 5. Wavelength and bandwidth stability for three systems in the Wafer Simulation Test, demonstrating stable and consistent system performance for 90W and 120W power modes across lot-to-lot power switching.

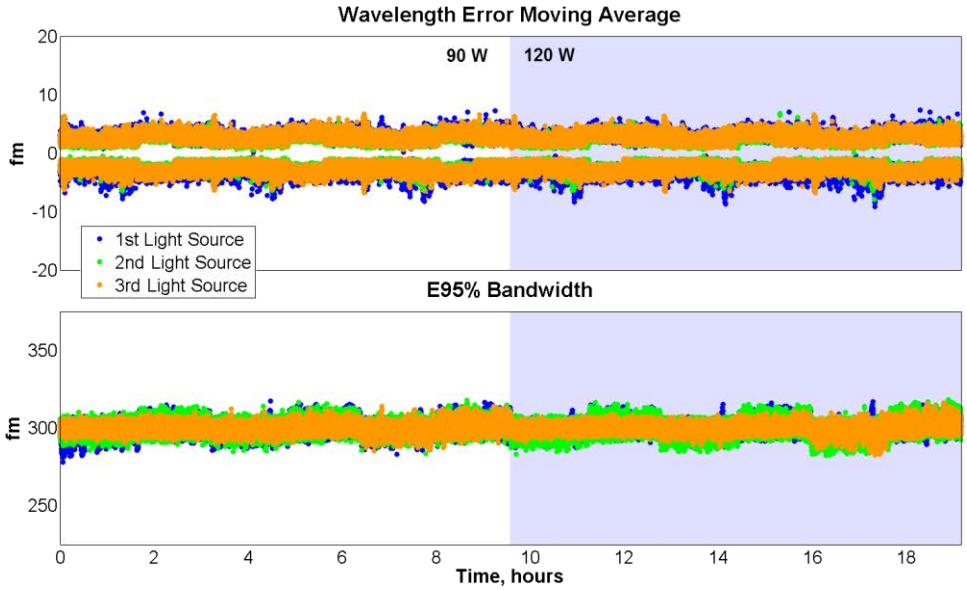

Figure 6. Wavelength and bandwidth stability for three systems in the 20-Hour Endurance Test, demonstrating stable and consistent system performance for 90W and 120W power modes.

There are several additional light source performance metrics of concern to chipmakers in addition to dose stability, wavelength stability, and E95% bandwidth stability shown in the previous figures for three 120W ArFi systems. A previous article on the 120W ArFi light source includes data to demonstrate excellent beam polarization at the highest duty cycle and power output expected in field use [6]. This previous article also demonstrates stable beam divergence, beam width, beam pointing stability, and beam position stability up to 120W. These parameters were also monitored during the extensive design validation testing for three 120W ArFi systems, demonstrating stable and consistent performance up to 120W. For example, figure 7 shows beam divergence and pointing stability in two axes for three 120W ArFi systems in the Wafer Simulation Test, and figure 8 shows beam energy density in the 20-Hour Endurance Test as measured by two-dimensional beam imaging metrology.

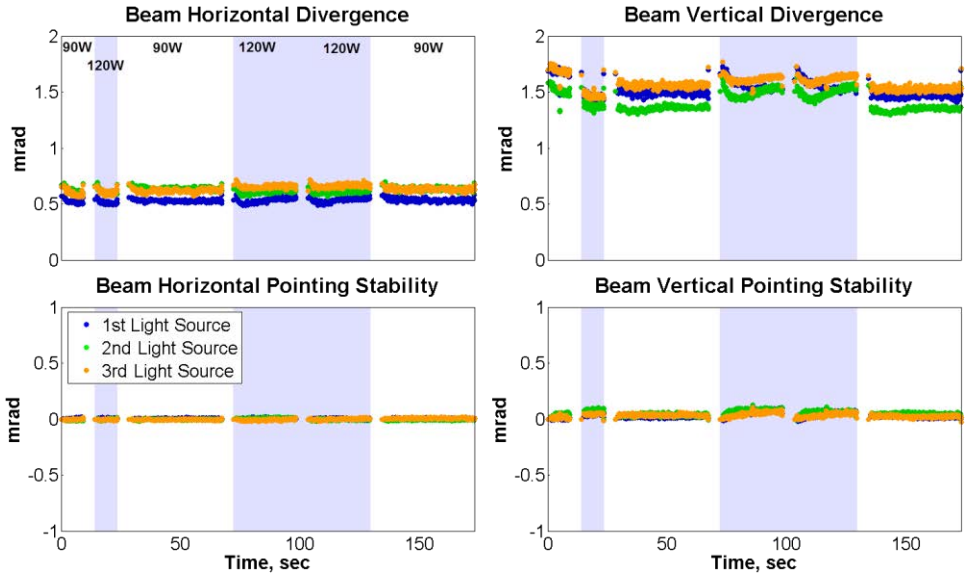

Figure 7. Beam divergence and pointing stability for three systems in the Wafer Simulation Test, demonstrating stable and consistent system performance for 90W and 120W power modes across lot-to-lot power switching.

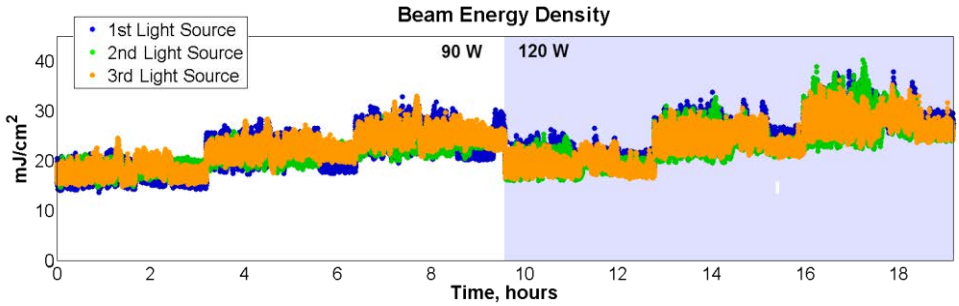

Figure 8. Beam energy density as measured by two-dimensional beam imaging in the 20-Hour Endurance Test, demonstrating stable and consistent system performance for 90W and 120W power modes.

4. SUMMARY AND CONCLUSIONS

Cymer has conducted a technology demonstration program to assess the key performance capabilities of a 120W ArFi light source to meet anticipated semiconductor industry requirements. Higher light source power is expected to be a future requirement to support 450mm wafer applications, high dose applications, and also high-throughput immersion and multiple-patterning applications. Flexible 90W to 120W output power with lot-to-lot power switching will enable optimized dose for a variety of lithography processes. As part of the technology program, three 120W demonstration units were built and tested. The test results indicated that the key optical parameters were stable across different power levels, and showed consistent performance across the multiple units. In addition, the demonstration units confirmed that wall-plug efficiency of the 120W lightsource was increased by 30% compared to the current XLR 600ix model, so that increased output power does not require any additional facilities power.

5. REFERENCES

1) D. Brown, et al., "XLR 500i: Recirculating Ring ArF Light Source for Immersion Lithography," Proc. SPIE Advanced Lithography 2007.

2) V. Fleurov, et al., "XLR 600i: Recirculating Ring ArF Light Source for Double Patterning Immersion Lithography," Proc. SPIE Advanced Lithography 2008.

3) R. Rokitski, et al., "Enabling High Volume Manufacturing of Double Patterning Immersion Lithography with the XLR 600ix ArF Light Source," Proc. SPIE Advanced Lithography 2009.

4) R. Rokitski, et al., "High Reliability ArF Light Source for Double Patterning Immersion Lithography," Proc. SPIE Advanced Lithography 2010.

5) T. Cacouris, et al., "Advanced Light Source Technologies that Enable High-Volume Manufacturing of DUV Lithography Extensions," Proc. SPIE Advanced Lithography 2012.

6) R. Rokitski, et al., "High Power 120W ArF Immersion Light Source for High Dose Applications," Proc. SPIE Advanced Lithography 2013.

Estimation of 1D Proximity Budget Impacts due to Light Source for Advanced Node Design

RC Peng[a], Tony Wu[a] and HH Liu[a]

[a]Taiwan Semiconductor Manufacturing Corp., Hsinchu Science Park, Hsinchu, Taiwan 300-77, R.O.C.

ABSTRACT

The laser impacts on the proximity error are well known in many previous studies and papers. The proximity budget control is more and more important for advanced node design. The goal of this paper is to describe the laser spectral bandwidth and wavelength stability contributions to the proximity budget by considering general line/space and trench pattern design. We performed experiments and modeled the photolithography response using Panoramic Technology HyperLith simulation over a range of laser bandwidth and wavelength stability conditions to quantify the long term and short term stability contributions on wafer-to-wafer and field-to-field proximity variation. Finally, we determine the requirements for current system performance to meet patterning requirements and minimize the laser contribution on proximity error and within 4% of target CD Critical Dimension Uniformity (CDU) budget process requirement [2]. This paper also discusses how the wafer lithography drivers are enabled by ArFi light source technologies.

Keywords: Proximity budget control, laser spectrum, photolithography simulation

1. INTRODUCTION

Advanced node designs require tighter process control, and especially the Critical Dimension Uniformity (CDU) error need to be controlled within 4% of target CD [2]. In order to achieve this, we have to more acutely maintain tight Iso-Dense Bias (IDB) control as part of the overall Optical Proximity Effect (OPE) portion of the Critical Dimension (CD) Budget. The laser bandwidth E95 is the one of the OPE contributors that need to be considered.

By studying through-pitch performance of line/space and trench pattern design which effect by laser bandwidth E95, we first performed lithography simulations to understand the CD error effect by bandwidth E95, and then verified the results by wafer exposure experiments. This enabled determining the CD error sensitivity as a function of changes to bandwidth E95.To determine the proximity budget contribution by laser performance variations, the wafer-to-wafer and field-to-filed performance during wafer exposures was analyzed for multiple systems using SmartPulse data collection. Based on the sensitivity of proximity variation, we could then quantify the laser population contributions to CD error variation for the current advanced design node. We also determined laser bandwidth E95 stability needed in order to meet the control requirements for the next generation advanced design node.

2. SIMULATION

2.1 Simulation Conditions

Figure 1. illustrates the binary mask Line/Space and Trench feature through pitch for the simple 1D design with pattern duty cycle up to 10 were simulated. For the semi-ISO and ISO pitch feature, sub-resolution assistant features (SRAFs) were used, and also mask biases were applied to compensate optical proximity effects. Figure 2. shows the two types of illumination conditions (193nm immersion + strong OAI illumination + Polarization) with Hyper-NA 1.35. In order to estimate the CD error response to bandwidth E95 changes, we used the Modified Lorentzian spectral approximations to generate the spectral profile as Figure 3. for Panoramic HyperLith simulation.

Figure 1. Feature from dense pitch to ISO with SRAF

For Line/Space For Trench

Figure 2. Illumination Settings

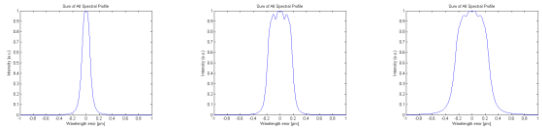

E95=300fm E95=450fm E95=600fm

Figure 3. Simulated Laser Spectral Profile for Various Bandwidth E95

2.2 Simulation Results

The figure 4.(a) and (b) shows the simulated CD error response to E95 bandwidth changes. An increase in E95 bandwidth leads to an increase in focus blur effect (or contrast loss) on the wafer. The pitch-A (Line/Space) or pitch-A' (Trench) is dense pitch; the pitch-I (Line/Space) and pitch-V' (Trench) are ISO pitches, therefore having larges impact on changes in CD. In general when bandwidth increases, the CD decreases most for the semi-ISO (forbidden pitch) and ISO pitch, which are structures also most sensitive to the contrast changes. All the pitches are referenced to the bandwidth E95 of 300fm, since this is the nominal set-point for XLR 660ix bandwidth control. We calculated the relative the CD error from the 300fm bandwidth E95 reference. From simulation result show, the pitch-C (Line/Space) and pitch-I' (Trench) are the most sensitive pitches to contrast or bandwidth E95 for these patterning conditions. For each pitch we normalized the CD error to the target CD for that pitch at the baseline bandwidth E95 of 300fm.

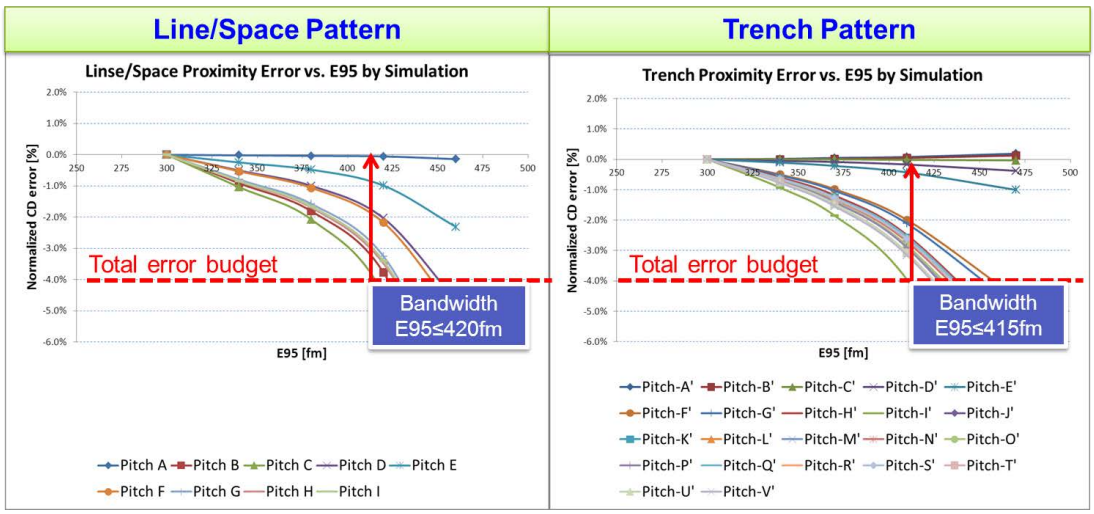

Figure 4. (a) Line/Space Simulation Result

Figure 4. (b) Trench Simulation Result

3. WAFER EXPERIMENT AND DISCUSSIONS

3.1 Wafer Experiment Conditions

Wafer exposure experiments were carried out to test Trench pattern response to changes in laser optical parameters, in order to determine the on-wafer bandwidth E95 response. As shown in Figure 5, we tested three E95 conditions with nominal E95 (292fm), setting-1(E95 = 385fm) and setting-2 (E95 = 475fm) on the XLR660 ix system. The actual laser performance during wafer exposure was obtained by using SmartPulse data collection, which enables collection of per

wafer laser beam and optical parameters during wafer exposure, as described in Figure 6. We measured the on-wafer CD through pitch by CDSEM, and obtained the exposure bandwidth E95 values for the actual wafers exposed to determine the direct correlation. The bandwidth E95 data reported in Figure 5, in this controlled experiment, are an average of all fields per wafer.

	Nominal	Setting 1	Setting 2
E95 [fm]	292	385	475

Figure 5. Bandwidth E95 Experiment Conditions

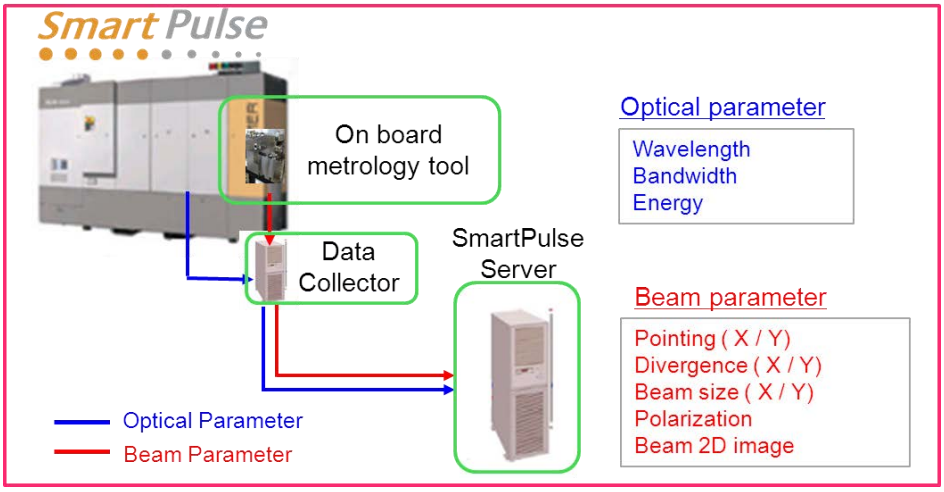

Figure 6. SmartPulse Data Collection Architecture

3.2 CD Results and Comparison

Figure 7. (a) shows the wafer experimental results for the Trench pattern CD error vs. bandwidth E95for various pitches. Comparing to pervious Trench simulation results, the simulation trend is consistent with the wafer experiment; the pitch-I' is the critical pitch to limit the bandwidth E95, and it needs to be controlled within 415fm (by simulation) or 430fm (by wafer experiment) to ensure the proximity error with 4% of target CD. We can calculate the contribution of laser bandwidth E95 variation to proximity budget from the ΔCD / ΔE95 error sensitivity.

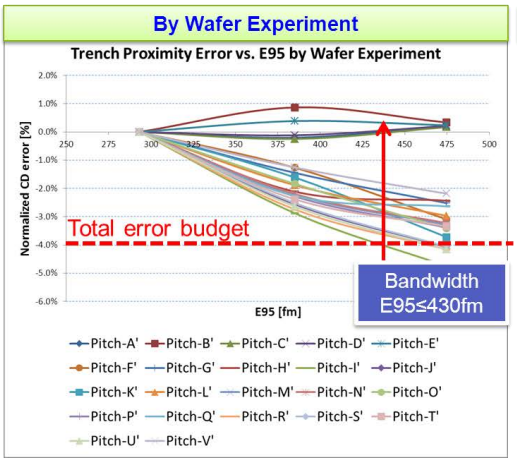

Figure 7. (a) Trench wafer experiment result

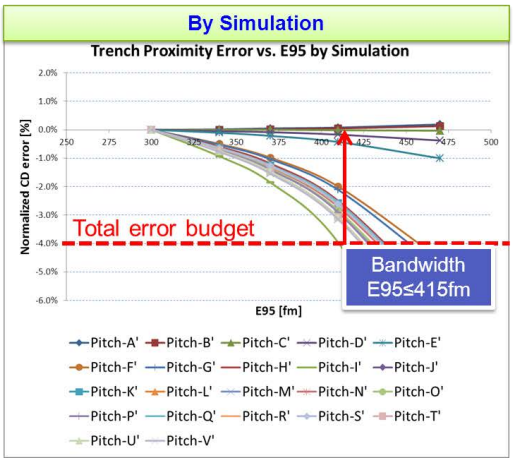

Figure 7. (b) Trench simulation result

3.3 Quadratic Fitting for Bandwidth E95 Sensitivity

Based on the agreement of Trench wafer experiment and simulation result, we take the most sensitive pitches, pitch-C (Line/Space) from simulation result and pitch-I' (Trench) from simulation and experiment result to calculate the bandwidth sensitivity. The bandwidth impact on CD can be described by a polynomial fit of second order, which will enable determining the ΔCD / ΔE95 sensitivity. Therefore we use the following quadratic curve fitting, $\Delta CD = a * \Delta E95^2 + b * \Delta E95 + c$. ……. (eq 1.) to the simulation and experiment data. Figure 8.(b) shows the Trench pitch-I' quadratic fitting result; the wafer experiment and simulation results are matched and follow the quadratic fitting curve very well. For bandwidth E95 variation within 100fm, the quadratic fitting curve should accurately correspond to the measured proximity error response. Figure 8.(a) also illustrates the Line/Space pitch-C quadratic fitting result, we assume the simulation result can represent of the real case, since wafer exposure data is not reported.

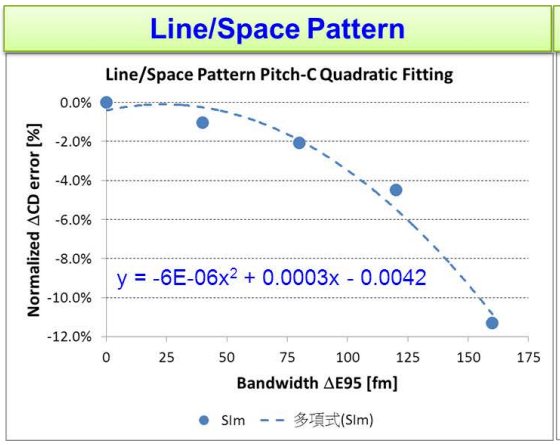

(a) Line/Space pitch-C

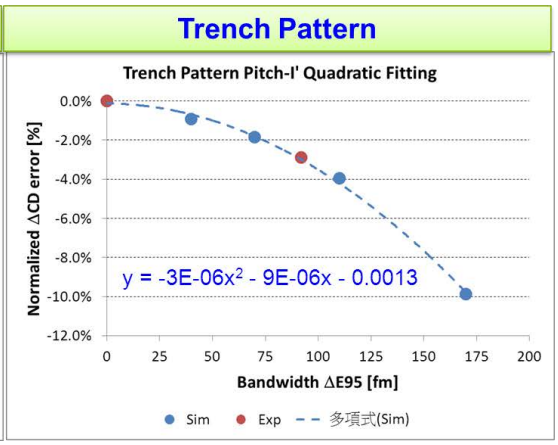

(b) Trench pitch-I'

Figure 8. The bandwidth CD sensitivities of Line/Space and Trench

4. LASER BANDWIDTH POPULATION FROM INSTALLED SYSTEM

4.1 Characterize the Bandwidth Variation

In previous discussion, we collected bandwidth E95 variation (standard deviation) and mean across the wafer during wafer-exposure by SmartPulse data collection in order to characterize the short-term and long-term stability performance

of installed systems. The total E95 variation can be estimated by adding the E95 intra-wafer variation from field-to-field data (short-term) and wafer-to-wafer (long-term) variation, and then calculating the total E95 variation by RSS (root sum square):

$$E95_{3\sigma\,total} = \sqrt{(E95_{3\sigma\,F2F})^2 + (E95_{3\sigma\,W2W})^2} \quad \text{……..(eq 2.)}$$

Where

$E95_{3\sigma\,total}$: Overall bandwidth E95 variation

$E95_{3\sigma\,F2F}$: Field to field bandwidth E95 variation (short-term)

$E95_{3\sigma\,W2W}$: Wafer to wafer bandwidth E95 variation (long-term)

4.2 Installed Laser Systems Bandwidth Population

In order to determine the nominal performance of bandwidth E95 variation across a population of tools, we collected the six XLR 660ix installed systems performance over 1 month production operation by using SmartPulse data collection to determine the performance levels delivered on-wafer. Figure 9. shows trend plots of bandwidth E95 performance for six systems. The blue dots show the intra-wafer bandwidth E95 1sigma calculated from bandwidth E95 data per exposure field; this is referred to as field-to-field bandwidth E95 variation. The green dots are average bandwidth E95 per wafer. Therefore the long-term (1 month) field-to-field and wafer-to-wafer variation can be estimated by calculating the standard deviation field-to-field data and wafer-to-wafer data across the installed systems.

Figure 10. shows the performance of bandwidth E95 across six systems for field-to-field and wafer-to-wafer variation . The Tool-E has the largest field to field bandwidth E95 variation around 30fm, while Tool-B has the largest wafer-to-wafer bandwidth E95 variation around 35fm. Overall Tool-B has the largest overall total bandwidth E95 variation around 40fm.

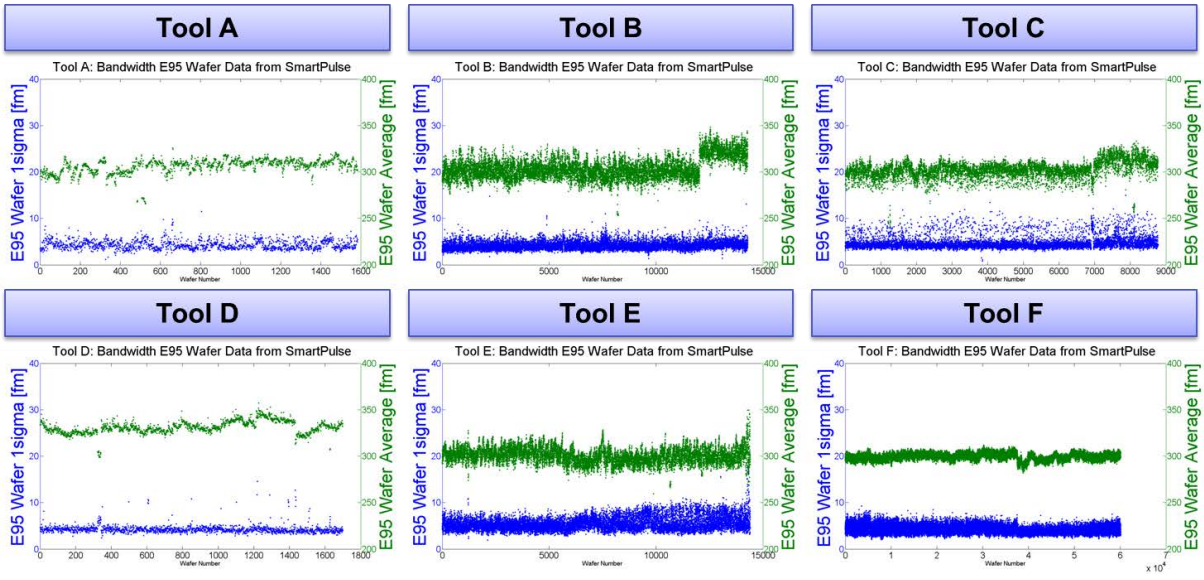

Figure 9. XLR660 ix Installed-system Bandwidth E95 monitoring trends over 1 Month by SmartPulse data collection

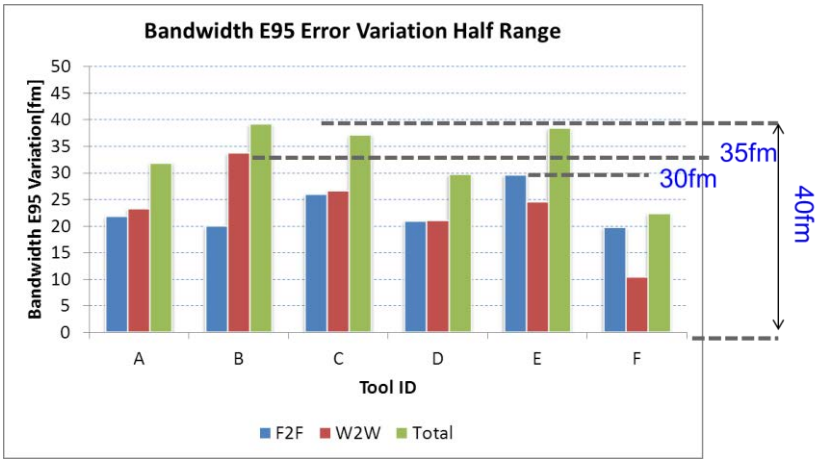

Figure 10. XLR 660ix Installed-system Bandwidth E95 Variation Estimate

4.3 Proximity Variation Estimated

Taking the critical pitch bandwidth E95 sensitivity from section 3.3and the tool bandwidth E95 variation from section 4.2, the proximity variation due to bandwidth E95 performance can be obtained by (eq 1.). Figure 11. (a) shows the Line/Space feature CD proximity field-to-field (F2F), wafer-to-wafer (W2W) and overall variation; the worst case total variation is around 0.53% of target CD. Figure 11. (b) shows the Trench feature CD proximity field-to-field (F2F), wafer-to-wafer (W2W) and overall variation, with worst case total variation around 0.67% of target CD.

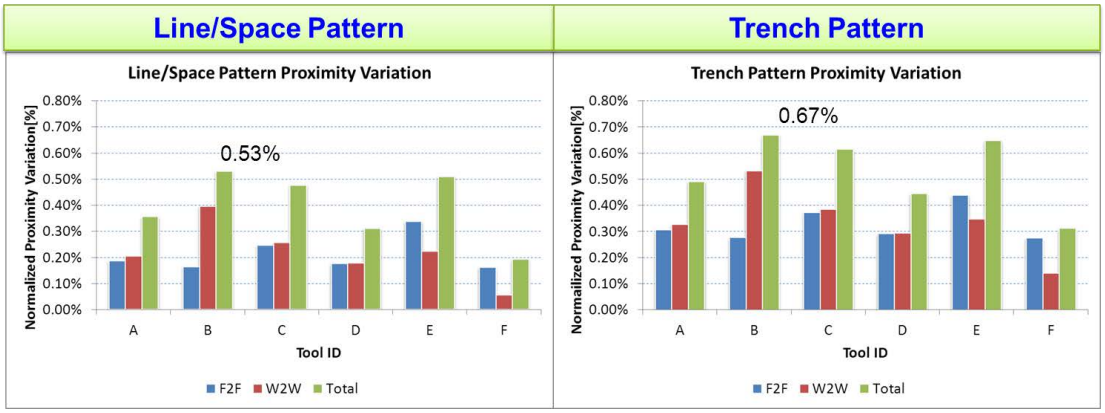

Figure 11. (a) Line/Space proximity variation

Figure 11. (b) Trench proximity variation

4.4 Next Advanced Design Node Laser Bandwidth Stability Requirement

As stated previously, for the advanced node design considered in this paper, the proximity contribution by laser bandwidth E95 of current XLR 660ix systems can be 0.67% of target CD. If we assume that the next generation design node requires reducing the CDU budget by half of current node, therefore, in order to keep the same laser bandwidth E95 contribution to proximity CD variation, total (field-to-field and wafer-to-wafer) worst case bandwidth E95 variation of 20fm is required for next generation lasers.

5. CONCLUSION

For the current advanced node design, the total XLR 660ix laser bandwidth E95 variation (field-to-field and wafer-to-wafer), estimated using data from actual wafer exposures using SmartPulse date collection, can contribute ~0.67% of target CD for total bandwidth E95 variation operating at nominal performance. In order to meet the next generation node requirements, assuming half of the total CDU budget of current design node, bandwidth stability within 20fm is required.

ACKNOWLEDGMENT

We thank Simon Hsieh, Ivan Lalovic and Omar Zurita at Cymer for laser perturbation experiment and data collection works that facilitated every scheduled test step of this project.

REFERENCE

[1] Rudy Peeters et al., " *ASML's NXE platform performance and volume introduction* ", *Proc. SPIE*8679, Extreme Ultraviolet (EUV) Lithography IV, 86791F (April 1, 2013)

[2] Jo Finders et al., "*Solutions for 22-nm node patterning using ArFi technology*", *Proc. SPIE* 7973, Optical Microlithography XXIV, 79730U (April 05, 2011)

[3] R. C. Peng et al. "Laser spectrum requirements for tight CD control at advanced logic technology nodes", *Proc. SPIE* 7640, Optical Microlithography XXIII, 76402C (March 03, 2010)

[4] T. Oga et al., "*Challenging to meet 1nm Iso- Dense Bias (IDB) by controlling Laser Spectrum*", Advanced Lithography XXI, SPIE 6520-144 (2007)

[5] K. Yoshimochi et al., "*32nm Node Device Laser-bandwidth OPE Sensitivity and Process Matching*", Optical Microlithography XXI, SPIE 7274-115 (2009)

[6] K. Yoshimochi et al., "*45nm Node Logic Device OPE Matching between Exposure Tools Through Laser Bandwidth Tuning*", Optical Microlithography XXI, SPIE 6924-92 (2008)

[7] Lalovic et al., "*Defining a physically-accurate laser bandwidth input for optical proximity correction (OPC) and modeling*", Proc. BACUS XXII Photomask Technology Symposium 7122-62, (2008)

[8] L. Van Look et al., "*Tool-to-tool optical proximity effect matching*;" Proc. SPIE. 6924, Optical Microlithography XXI 69241Q (March 14, 2008)

Improvements in Bandwidth & Wavelength Control for XLR 660xi Systems

Will Conley, Hoang Dao, David Dunlap, Ronnie Flores, Matt Lake, Kevin O'Brien, Alicia Russin, Aleks Simic, Joshua Thornes, Brian Wehrung, John Wyman

Cymer Inc., 17075 Thornmint Ct., San Diego, CA, 92127, USA

Abstract

As chipmakers continue to reduce feature sizes and shrink CDs on the wafer to meet customer needs, Cymer continues developing light sources that enable advanced lithography, and introducing innovations to improve productivity, wafer yield, and cost of ownership. In particular, the architecture provides dose control and improved spectral bandwidth stability, both of which enables superior CD control and wafer yield for the chipmaker.

The XLR 660ix incorporates new controller technology called ETC for improvements in spectral bandwidth stability, energy dose stability, and wavelength stability. This translates to improved CD control and higher wafer yields. The authors will discuss the impact that these improvements will have in advanced lithography applications.

1. Introduction

Double-patterning ArF immersion lithography continues to advance the patterning resolution and overlay requirements and has enabled the continuation of semiconductor bit scaling. Over the years, Lithography Engineers continue to focus on CD control, overlay and process capability to meet current node requirements for yield and device performance. Reducing or eliminating variability in any process will have significant impact, but the sources of variability in any lithography process are many. The goal from the light source manufacturer is to further enable capability and reduce variation through a number of parameters. Table 1 summarizes the lithography parameter and the light source requirement. [1, 2, 3, 4]

Table 1

Litho parameters	Light source requirements
Contrast, CD Control	Bandwidth control & stability
Dose Control	Energy control & stability
Focus, Overlay	Wavelength control & stability

2. What is ETC?

ETC is a collection of new algorithms for XLR660ix light sources that execute in real time to tightly control the system's energy and dose, central wavelength, and spectral bandwidth. These algorithms comprise linear and nonlinear elements, adaptive feedback and feed-forward, multivariable architectures, and specialized knowledge bases earned through Cymer's years of light source research and development. Under tightening requirements for next generation scanners, the new algorithms instantiate advanced actuation techniques to improve speed and accuracy. However, these techniques also increase the complex coupling between the various light source subsystems. Additionally, the effects of exogenous disturbances – previously rejected through straightforward feedback – became a significant fraction of the requirements

budget. Therefore, the algorithms also needed to decouple disparate parameter interactions, and simultaneously precisely characterize and fully reject the largest disturbances. The result is a tightly interacting high performance controller able to achieve the necessary improvements without any changes to XLR660ix hardware.

More academically, the design of ETC deeply understands the light source's dynamics and disturbances. It uses this to push its model-based feedback designs to the edge of robust stability limits. It also incorporates advanced adaptive and learning techniques to further push performance bounds while maintaining stability. For example, the effects of firing duty cycle on performance parameters are known to vary over time and between systems; the ETC algorithms adapt models of these effects to the current time and system and apply the model to improve control. ETC is therefore more than a set of algorithms; it is the application of the accumulation of systems knowledge coupled to advanced methods to deliver the tight control in energy, wavelength, and bandwidth that the next generation scanners need.

3. Improved Stability Control

Figure 1 is a diagram of the XLR 660ix system highlighting the location of the line-narrowing module (LNM), the master oscillator (MO) and power ring amplifier (PRA), the pulse power modules and new software to enable algorithms in the light source. There are no changes in the current hardware design of the light source to enable these improvements.

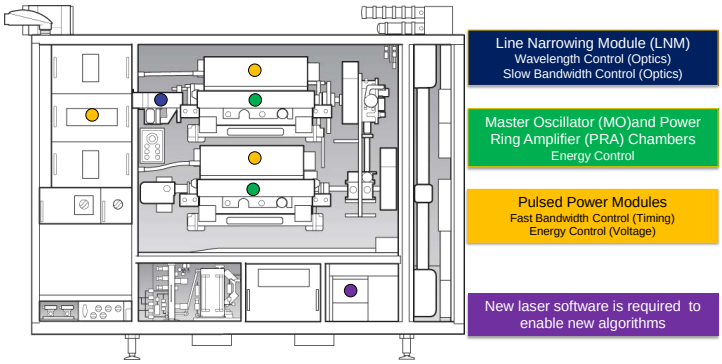

Figure 1

4. Results & Discussion

   a. Bandwidth Stability

To achieve ever-increasing demands of contrast and CD control, stability of spectral bandwidth is essential. With introduction of ETC we now control the spectral bandwidth pulse by pulse. This enables us to maintain the bandwidth mean to within ±3fm of the target as shown in Figure 2. Also shown is legacy bandwidth performance, which clearly illustrates the leap in performance brought by ETC.

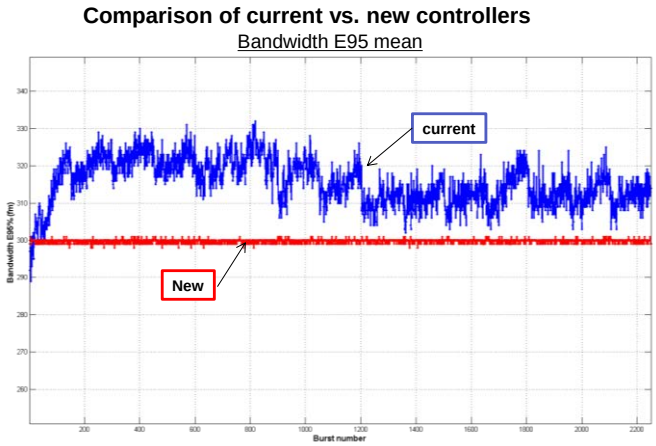

Figure 2 – Enhanced bandwidth stability enables improved CD uniformity

As inherent bandwidth disturbances of light source are hardware dependent, they differ in magnitude and severity from system to system. This is the reason that ETC's adaptability and learning ability, discussed in Section 2, play a key role in maintaining the same level of performance on different systems. In Figure 3 we show bandwidth mean (top plot) and die minimum/maximum values (bottom plot) for nine ETC systems currently in the field. Data is taken using simulated wafer-exposure firing pattern, and it includes 2250 dies. It is clear that mean bandwidth is kept within ±3fm of the target, with extreme values in die reaching ±12 fm. This clearly shows robustness and repeatability of ETC bandwidth control.

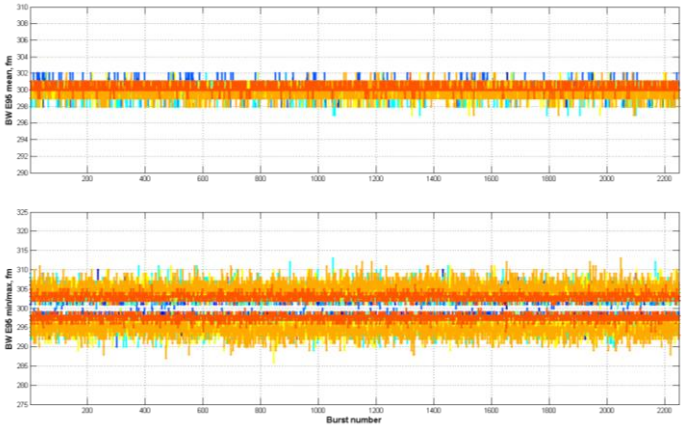

Figure 3 – Bandwidth control over 9 systems currently in the field

b. Wavelength Stability

Scanner stage speeds continue to increase to support the higher throughput demands of chipmakers. Scanner focus and overlay requirements are tightening. To the light source, a higher stage speed corresponds to fewer pulses which can be used for control purposes as the imaging slit passes across the exposure field, and tighter focus and overlay requirements imply the light source wavelength stability needs to be tighter Cymer has introduced a new wavelength controller with the ETC which improves wavelength stability performance even with >25% reduction in the number of pulses averaged by the slit. This controller continually

predicts the inherent light source disturbances and the physical state of the wavelength actuators, and uses optimal feedback control methodology to provide the highest level of wavelength control performance Cymer has ever achieved. A comparison of our previous controller and the ETC wavelength controller performance is provided in Figure 5. Both of the wavelength metrics (average error and moving sigma) commonly used to characterize wavelength stability of a DUV light source show significant improvement. Enhanced wavelength stability enables improved CD uniformity with slit reduced by 25%.

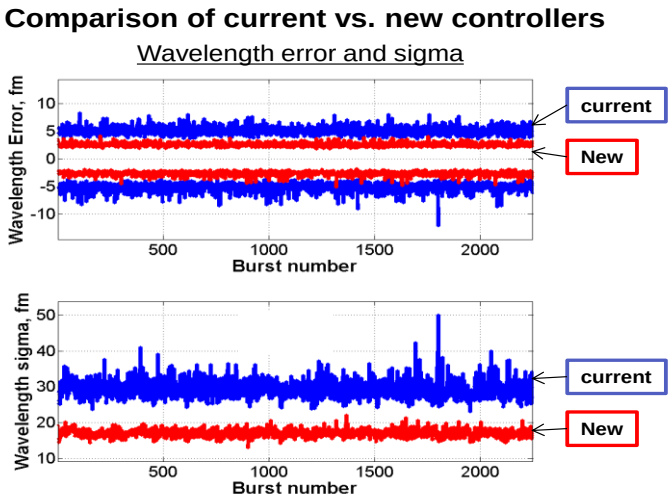

Figure 4

c. Dose Stability Performance

Similarly, to wavelength, the increased stage speeds also are demanding on the dose control that the light source provides. The dose controller also is coupled into other ETC controllers for bandwidth. These two factors required advanced solutions for dose control to maintain the high level of performance expected by chipmakers, which the Cymer light source is able to provide with the introduction of ETC. Slit size reduce by 25% with no performance penalty. BW & WL stability requirements were achieved with no impact to dose stability

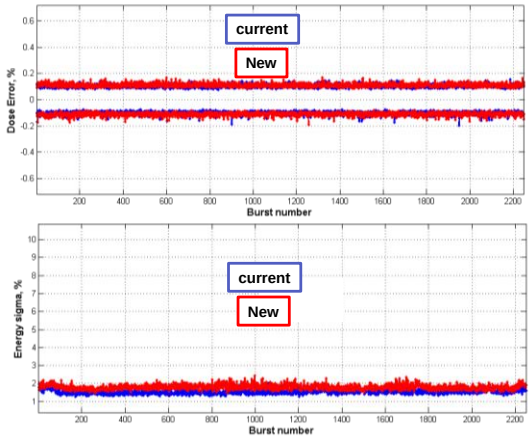

Figure 5

5. Conclusions

In this paper, the Authors have demonstrated a new controller technology for improvements in spectral bandwidth stability, energy dose stability, and wavelength stability. We have demonstrated performance over multiple systems, which have been deployed at multiple chipmakers. This performance will translate into improved CD control and higher wafer yields. ETC offers substantial improvement in both wavelength & bandwidth control, as well as improvements to energy control to allow operation with the slit reduced by up to 25%. ETC algorithms have been deployed next generation scanners and have demonstrated real improvements, which can be made by algorithm only changes rather than hardware development.

6. References

1. I. Lalovic et al., Defining a physically-accurate laser bandwidth input for optical proximity correction (OPC) and modeling, Proc. BACUS XXII Photo mask Technology Symposium 7122 - 62, (2008).
2. P. De Bisschop et al., Impact of finite laser bandwidth on the CD of L/S structures, Journal of Micro / Nanolithography, MEMS and MOEMS (JM3), Vol. 7, No. 3, (2008)
3. M. Smith et al., Modeling and Performance Metrics for Longitudinal Chromatic Aberrations, Focus-drilling, and Z-noise; Exploring excimer laser pulse-spectra," Proc. SPIE Optical Microlithography XX 6520 -127 (2007)
4. U. Iessi et al., Laser bandwidth effect on overlay budget and imaging for the 45 nm and 32nm technology nodes with immersion lithography, Proc. SPIE Optical Microlithography XXIII 7640 (2010).

7. Acknowledgements

The authors acknowledge the contribution of the Test Engineering Team in San Diego, the Site Operations teams and the support of Management.